Controlling quantum correlations in optical-angle–orbital-angular-momentum variables

Yue Zeng,[*] Dongkai Zhang,[*] Fangqing Tang, Shaochen Fang, Wuhong Zhang,[†] and Lixiang Chen[‡]
Department of Physics, Xiamen University, Xiamen 361005, China

(Received 10 August 2021; accepted 9 November 2021; published 29 November 2021)

The entanglement of optical angular position and orbital angular momentum has become one of the important degrees of freedom for quantum information science. Quantum control of the two conjugate variables may provide a gate to control the production of the entanglement. Here, we theoretically and experimentally show that by controlling the transverse spatial coherence of the pump beam, one can modulate the strength of the quantum correlations between the angular position and orbital angular momentum in down-converted photon pairs. By determining the relation of the Einstein, Podolsky, and Rosen correlations with the transverse spatial coherence of the pump, the boundary of the entanglement can be determined. Our work shows that the transverse spatial coherence of the pump can act as a switch to control the production of quantum entanglement both for discrete and continuous conjugate variables and may provide another platform for the quantum control research field.

DOI: 10.1103/PhysRevA.104.053719

I. INTRODUCTION

Entangled photons have become a standard tool in quantum information [1] and foundations [2,3]. They have been explored to generate nonclassical correlations among different degrees of freedom, such as polarization [2–5], time and frequency [6–8], position and momentum [9], radial position and radial momentum [10], as well as angular position (ANG) and orbital angular momentum (OAM) [11,12]. In contrast with the linear momentum and position being simply Fourier transforms of each other for probability distributions, the angle is 2π periodic, and therefore bounded, so the angular variable is expressed as a discrete and unbounded Fourier series of angular momenta [13]. The discrete nature of OAM and the continuous but periodic nature of ANG provides a special sort of entanglement between these two variables. The study of the uncertainty relation [14], Fourier relation [15], and the Einstein-Podolsky-Rosen (EPR)-Reid criterion [12] between the OAM and ANG paves the way to real quantum information applications. For example, an efficient method was proposed for sorting both the OAM and ANG modes for quantum information [16], a high-dimensional quantum key distribution scheme was implemented by using ANG and OAM [17], and another way to directly measure a 27-dimensional OAM state vector was proposed through weak measurements of OAM and strong measurements of ANG [18]. All of the above studies have shown that the entanglement of optical ANG and OAM has become one of the important degrees of freedom for quantum information science. However, only a small amount of research has been focused on how to control the quantum entanglement of the two variables.

In order to control a quantum system, one essential way is to control the generation process. As have well been studied, ANG-OAM entangled photon pairs are often generated by spontaneous parametric down-conversion (SPDC) [12,15,17,18]. The SPDC process is usually driven by a pump beam with transverse spatial coherence, whose profile not only determines the quality of entanglement [9,19], but also the transverse structure of the generated photons [20–23]. Recent years have witnessed a growing interest in modulating the transverse structures of the pump beams to control the production of the desired entangled photon pairs. By introducing a π-phase step to the transverse profile of the pump, Remero *et al.* observed a modulation of the ANG correlations consistent with the Fourier relationship between the OAM and angle [24]. They further implemented a tunable high-dimensional OAM entanglement by tuning the phase matching in the SPDC process [25]. More recently, by shaping the spatial profile of the pump, spatial Bell-state generation without transverse mode subspace postselection [26,27], OAM-entangled state engineering [28–31], and spatial entanglement engineering [32,33] have been extensively proposed. When considering the Fourier spectrum of the OAM modes in the pump beam, an interesting quantum pattern recognition scheme was realized recently [34].

However, all of the above-mentioned methods have focused on controlling the transverse profile of the pump, and in fact, it is not the pump profile that is relevant to the joint transverse distribution of the signal and idler, but its angular correlation function, which means that the transverse spatial coherence of the pump field is crucial in determining the degree of entanglement of the generated signal and idler photons. There were some early attempts to theoretically study the transfer of the spatial pump coherence to the down-converted photon pairs in Refs. [35–39]. By using a partial spatially coherent pump beam, the generation of entangled photon pairs has been implemented experimentally [40,41]. More recently, it was demonstrated theoretically that when pumping

[*]These authors contributed equally to this work.
[†]zhangwh@xmu.edu.cn
[‡]chenlx@xmu.edu.cn

by a twisted Gaussian Schell-model beam, the effect of the amount of entanglement increases inversely with the degree of coherence [42]. An incoherent light-emitting diode (LED) pump beam [43,44] was used to produced correlated photon pairs and then experimentally examined in the generation of position-momentum entanglement [45]. However, little attention has been paid to using the transverse spatial coherence of the pump to control the ANG-OAM entanglement in down-converted photon pairs. In this paper, we theoretically and experimentally show that by controlling the pump transverse coherence, one can modulate the strength of the quantum correlations between the ANG and OAM. For that, we pump a nonlinear crystal with a pseudothermal light of variable coherence lengths. By showing the value of the EPR correlations between ANG and OAM variables, we find that the strength of the OAM correlation depends strongly on the transverse spatial coherence of the pump but not the ANG, so that the degree of entanglement between the two conjugate variables can be controlled. Our results shed light on entanglement generation and can be applied to control the entanglement of other degrees of freedom for quantum information applications. Moreover, recent studies have experimentally demonstrated that the photon pairs generated using a partially spatial coherent pump are more robust towards varying atmospheric turbulence strengths than the photon pairs produced by a fully spatial coherent pump beam [46]. Thus our work may find important applications in free-space quantum communication using spatially entangled photons.

II. THEORETICAL ANALYSIS

It is known that under the condition of narrow aperture measurements, the EPR-Reid criterion of ANG and OAM conjugate variables can be denoted as a violation of the inequality [12]

$$(\Delta\ell_j)^2(\Delta\varphi_j)^2 \geqslant 1/4, \tag{1}$$

where ℓ_j is the quantum number of OAM, φ_j is the angle of the signal or idler photon, and $\Delta\ell_j$, $\Delta\varphi_j$ denote the variance of the OAM and ANG, which can be deduced by the joint probability distribution of OAM, $P(\ell_i, \ell_i)$, and ANG, $P(\varphi_i, \varphi_s)$. The simultaneous strong ANG and OAM correlations are a signature of entanglement. How to deduce the influence of the pump transverse spatial coherence on the joint probability distribution of OAM and ANG is our key point to control the degree of entanglement. We have recently demonstrated theoretically and experimentally that the transverse position correlations are independent of the transverse spatial coherence of the pump beam while the anticorrelations in momentum are crucially dependent on it [36,45]. As far as we know, few researchers have studied the influence of the pump transverse coherence on the correlation of ANG and OAM of the down-converted photon pairs. Here, we use a monochromatic Gaussian Schell-model beam [47] under the paraxial approximation to deduce this relation. First, we started on the derivation of the biphoton density matrix of ANG based on the coordinate transformation. Our detailed derivation processes are shown in Appendix A. The joint probability distribution

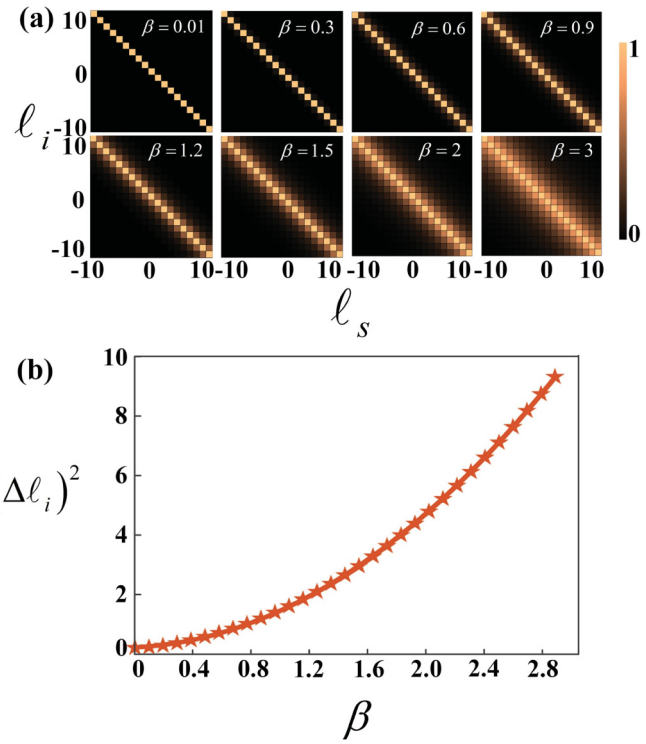

FIG. 1. (a) The analytical plots of the OAM joint probability distribution of photon pairs with different pump transverse coherences. (b) The numerical plot of the variance of OAM of idler photons with different pump transverse coherences.

of the ANG of biphotons is obtained as

$$P(\varphi_s, \varphi_i) = \frac{A(A-B)\sqrt{B/L}}{4\alpha(A+B)[A-B-(A+B)\cos(\varphi_s-\varphi_i)]}. \tag{2}$$

Here, we simplified this expression as $A = 32w^2\alpha k_p$, $B = L(1+4\alpha^2)$, where w is the pump beam waist, k_p is the wave number of the pump, L is the length of crystal, and the term α is responsible for the so-called walk-off and is usually defined as $\alpha = 0.455$ as a common choice [23]. From Eq. (2), we find that the joint probability distribution of ANG is independent of the pump transverse-coherence length of l_c and the ANG of the signal and idler photons is always correlated, in that correlation exists even for an incoherent pump. So the variance of the joint probability of ANG should be a constant along with the different pump transverse coherences theoretically.

For the joint probability distribution of OAM, we can expand the density matrix of ANG into OAM space. The detailed derivation processes are shown in Appendix B. The joint probability distribution of OAM of biphoton pairs is

$$\tilde{P}(\ell_s, \ell_i) = \frac{\sqrt{1-4\xi^2}}{1+2\xi}\left(\frac{2\xi}{\sqrt{1-4\xi^2}+1}\right)^{|\ell_s+\ell_i|}, \tag{3}$$

where $\xi = \frac{\beta^2}{1+2\beta^2}$ is just for convenient notation, and $\beta = w/l_c$ is used to describe the pump transverse-coherence property. It is noted that ξ and β are both relevant to the beam waist w and the transverse-coherence length l_c of the pump. The theoretical plots of the OAM joint probability distribution of photon pairs with different β are illustrated in Fig. 1(a).

In our simulation, we assume the system works in a perfect phase-matching condition. β ranges from 0.01 to 3, which can be used to represent the pump beam changing from a laser to nearly transverse-incoherent beam. As can be seen in Fig. 1(a), the joint probability distribution of OAM is well anticorrelated with small β, but becomes uncorrelated when β is large. So, by modulating the pump transverse-coherence length l_c with a fixed pump beam waist, one may modulate the degree of anticorrelation of OAM.

By projecting the OAM of signal photons on the special state, such as l_0, one can obtain the conditional probability distribution of OAM as $\tilde{P}(\ell_i|\ell_s = l_0)$. Here, we project the signal photon state into a zero OAM state based on the pump beam. So the variance of the conditional probability of OAM can be calculated by $(\Delta\ell_i)^2 = \sum_{\ell_i} \ell_i{}^2 \tilde{P}(\ell_i|\ell_s = 0) - [\sum_{\ell_i} \ell_i \tilde{P}(\ell_i|\ell_s = 0)]^2$. Based on Eq. (3), we obtain the variance of the idler photon,

$$(\Delta\ell_i)^2 = \frac{2\beta^2(1+2\beta^2)}{1+4\beta^2}, \tag{4}$$

Apparently, the variance is determined by the transverse-coherence length and inversely proportional to the square of the transverse-coherence length, as illustrated by the numerical plots in Fig. 1(b). One can clearly see that the variance increases quadratically with the β, which means that the joint probability distributions of OAM are dispersed increasingly with a decrease of the pump transverse-coherence length l_c.

Hence, from Eqs. (1), (2), and (4), one can deduce that with a partially transverse-coherent pump beam it becomes increasingly difficult to fulfill the requirements of the EPR-Reid criterion so that the entanglement can no longer be verified. However, it is this characteristic that guarantees our key idea to control the ANG-OAM entanglement by using the pump transverse-coherence modulation technique.

III. EXPERIMENTAL RESULTS

Our experimental setup is shown in Fig. 2. To generate a pseudothermal pump beam, we use a laser diode module impinging on a spatial light modulator (SLM1). It modulates the transverse phase profile of the beam and can be programed to simulate different transverse-coherence lengths [48]. The resulting beam with a waist of $w = 0.5$ mm illuminates the nonlinear crystal, which is a 1 mm × 2 mm × 5 mm periodically poled potassium phosphate (ppKTP) crystal. It produces degenerate down-converted photon pairs at 810 nm under collinear type-II phase-matching conditions, each consisting of a signal and idler photon that differ in polarization. A long-pass filter and a 10-nm spectral filter at 810 nm after the crystal block the pump beam and ensure the detection of frequency-degenerate photons. Signal and idler photons are separated by a polarizing beam splitter (PBS). Each one of them is imaged from the output facet of the crystal through a $4f$ system (with $f_1 = 50$ mm and $f_2 = 300$ mm) onto a second spatial light modulator (SLM2). To independently project the signal and idler on different modes, SLM2 is divided into two parts. Another $4f$ system (with $f_3 = 750$ mm and $f_4 = 2$ mm) reimages the modulated signal and idler photons onto the input facet of two single-mode fibers (SMFs). We display the desired holographic gratings on SLM2 to measure

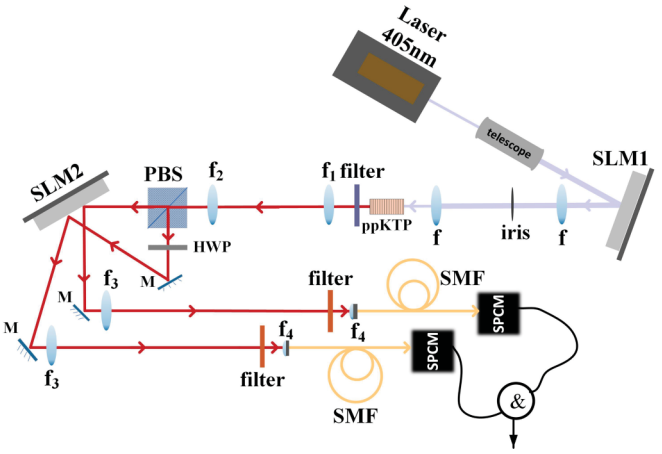

FIG. 2. Experimental setup. Photon pairs are generated by pumping the ppKTP crystal with a regulable transverse-coherence laser beam which is tuned by modulating the transverse phase profile with the SLM1, a polarization beam splitter (PBS) splits photon pairs into two paths, each of them illuminating onto the SLM2, and the joint probability distributions are measured by a combination of SLM2, a single-mode fiber (SMF), and avalanche photodiode single-photon counting modules (SPCM).

the angular positions and orbital angular momenta of the photon pairs. Photons passing through the fibers are detected by the avalanche photodiode single-photon counting modules (SPCMs), whose output is fed into a coincidence circuit. Only Gaussian modes can be coupled into the SMF so that, together with the grating of SLM2, it projects the incoming photons onto the desired ANG and OAM states.

To measure the joint probability distribution of ANG and OAM with different transverse-coherence lengths of the pump, SLM1 imprints different random phase patterns. The time interval of different random phase patterns is set to 0.3 s. For each data collection with 90 s integration, there are almost 300 random phase patterns. The statistics of these random patterns are Gaussian with a transverse width in the crystal of $\delta\phi = 0.6$ mm. By controlling the strength of the modulation depth ϕ_0, we can tune the coherence length $l_c = \delta\phi/\phi_0$ [45,48]. We vary the modulation depth from 0.001 to 8 to define a series of coherence lengths, and the coherence length roughly ranges from 0.1 to 600 mm, which represents the pump beam changing from an incoherent beam to a laser beam.

To measure the joint probability distribution of ANG, we use an angular sector transmission aperture programed by a hologram. The aperture is a Gaussian profile whose width θ and orientation φ can be changed. It is noted that what we should measure is the angular positions of photons, which just an orientation with a tiny width, so, the narrower the aperture, the more precise measurement of ANG can be obtained, but the photon counts will be too weak to measure with a narrow aperture. So in our experiment we set the angular aperture with a width of $\theta = 2\pi/15$ to get an appropriate signal under our pump transverse-coherence modulation.

For each central position φ_s of the angular aperture placed in the signal arm, we scan the central position φ_i of the angular aperture defined in the idler arm. By scanning φ_s and φ_i both

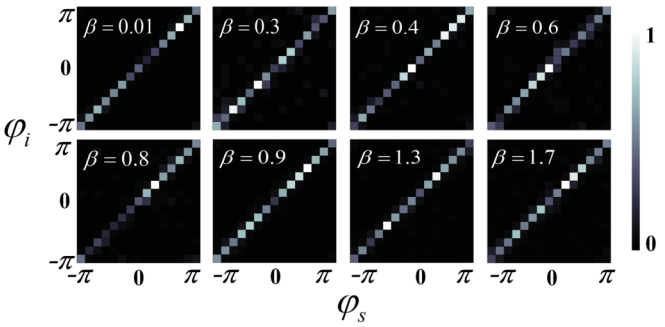

FIG. 3. Experimental results for angular position correlations with different pump transverse coherences. The joint probability distribution of ANG with $\beta = w/l_c$ changes from 0.01 to 1.7, which represents the pump beam changing from a laser to a nearly transverse-incoherent light. The integration time of each position is 90 s, and is averaged three times.

in the range from $-\pi$ to π with an interval of $\Delta\varphi = \theta$ with different pump transverse-coherence lengths, we obtained a series of the ANG distribution $P(\varphi_s, \varphi_i)$, as shown in Fig. 3. By changing β from 0.01 to 1.7, the joint probability distribution of ANG almost retains the same diagonal correlation, as predicted by our theoretical derivation in Eq. (2). The variance of ANG can then be obtained by using $(\Delta\varphi_i)^2 = \int d\varphi_i[|\varphi_i^2 P(\varphi_i|\varphi_s = 0)| - |\varphi_i P(\varphi_i|\varphi_s = 0)|^2]$. Here, we use the conditional probability of the ANG by considering the data of φ_i with $\varphi_s = 0$. It is noted that in our experimental measurements, the $\Delta\varphi$ is almost only one pixel size because of the limited angular aperture. So we expect that the real value of $\Delta\varphi$ should be smaller than our experimental calculation.

To observe the joint probability distribution of the OAM from the down-converted photon pairs, we prepare and display the desired holographic fork gratings on SLM2 to realize projective measurements of the OAM eigenstates. Similarly, for each OAM of the signal photons $\ell_s(-7 \to 7)$, we scan the idler photons ℓ_i from -7 to 7, and then obtain the probability distribution of OAM: $\tilde{P}(\ell_s, \ell_i)$. By varying the pump transverse-coherence lengths, we can get a series of $\tilde{P}(\ell_s, \ell_i)$, as shown in Fig. 4(a). Unlike the diagonal correlation of ANG, the OAMs are antidiagonal correlated when the pump transverse-coherence length l_c is very large (small β). However, as can be seen in the second row of Fig. 4(a), the anticorrelated feature of the OAM spectrum becomes broader with decreasing pump transverse-coherence length (increasing β), which means that the OAM antidiagonal correlation disappears. The experimental results coincide well with our theoretical plots in Fig. 1(a). Then, by considering the conditional probability $\tilde{P}(\ell_i|\ell_s = l_0)$, we can get the variances of OAM, as illustrated by the red triangle in Fig. 4(b). The blue curve is the theoretical plot with Eq. (4). One can see that the experimental results are well consistent with the theoretical calculation. The variances of OAM are just increased as quadratically with β, which is inversely proportional to the square of the pump transverse-coherence length. The feasibility of our key idea to control the correlation of OAM by modulating the transverse coherence of the pump beam has been well verified.

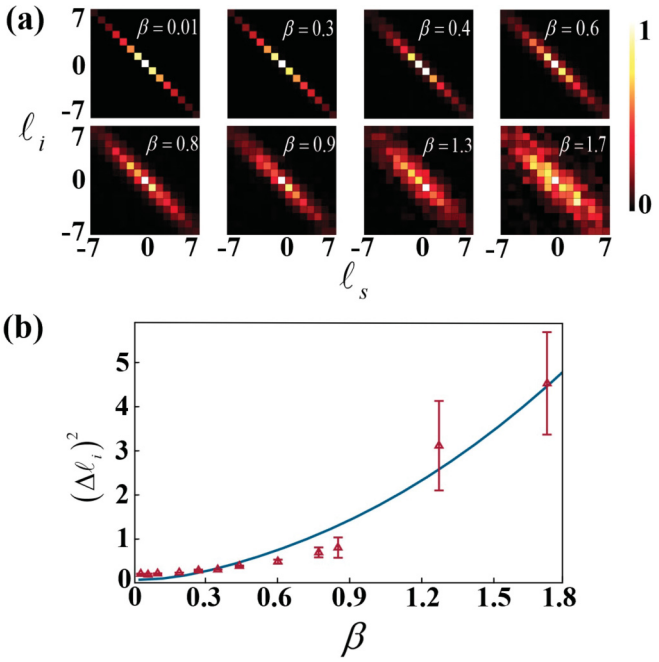

FIG. 4. Experimental results for orbital-angular-momentum correlations with different pump transverse coherences. (a) The joint probability distribution of OAM with $\beta = w/l_c$ changes from 0.01 to 1.7, which represents the pump beam changing from a laser to a nearly transverse-incoherent light. The integration time of each pixel is 60 s and is averaged three times. (b) The calculated value of the variance of OAM from the above results.

According to the EPR-Reid criterion of ANG and OAM conjugate variables as we mentioned in Eq. (1), we know that when the product of the variances of ANG and OAM exceeds the boundary (1/4) of the criterion, the entanglement of ANG-OAM disappears. By controlling the pump transverse coherence, we can actually implement a control of the quantum correlation of ANG and OAM. We show our results in Fig. 5, where the vertical axis of the graph describe the product of $(\Delta\ell_i)^2(\Delta\varphi_i)^2$, while the horizontal axis denotes the value of β. One can see that, for small β corresponding

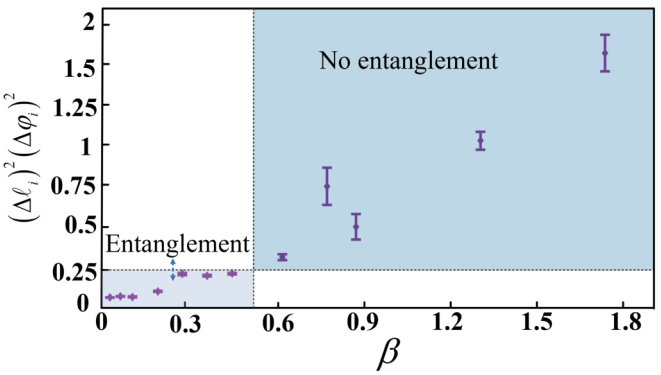

FIG. 5. Experimental results of the product $(\Delta\ell_i)^2(\Delta\varphi_i)^2$ with different pump transverse coherences. Their product increases with decreasing the coherence length until it exceeds the boundary, which below is a signature of quantum entanglement, and therefore makes the transition from entangled to classical correlated photon pairs.

to a large pump transverse-coherence length l_c, the product is below the boundary of the EPR-Reid criterion. The signature of violating the inequality means that the photon pairs are strongly correlated in ANG and OAM, so one can get the entangled state for further application. By increasing β (decreasing the pump transverse-coherence length), the product reaches and then exceeds the boundary, which means the correlation of OAM decreases and the entanglement of the ANG-OAM of photon pairs is no longer verified. Thus, the results shown in Fig. 5 clearly demonstrate that we have achieved control of the degree of entanglement of ANG-OAM conjugate variables. Quantum control of the entanglement of photon pairs can be achieved by varying the transverse-coherence length of the pump beam, which might provide a useful tool and robust technique for quantum information and technology.

IV. CONCLUSION

In conclusion, we have proposed and demonstrated a feasible way to control the entanglement of photon pairs in ANG and OAM conjugate variables. Controlling the correlation of ANG and OAM variables might provide "a gate" to control the information capacity for quantum information processing. Quantum control has attracted much attention due to its intrinsic relation to quantum-information-processing algorithms [49]. By shaping the classical laser beam, one can actually shape the single photons in real time by control and feedback [50]. Unlike the many quantum control works that are focusing on protecting the quantum system from decoherence [51], we actually use the coherence feature of the system and provide another platform for quantum control by controlling the transverse-coherence length of the pump. Our work might be combined with the well-known quantum feedback control theory [52] to provide an alternate technique that comes from source control to the exact preparation of a proper initial state for quantum information applications.

ACKNOWLEDGMENTS

We appreciate beneficial discussions with Professor Enno Giese of TU Darmstadt. This work is supported by the National Natural Science Foundation of China (12034016, 61975169, and 11904303), the Fundamental Research Funds for the Central Universities at Xiamen University (20720190054, 20720190057, 20720200074), the Natural Science Foundation of Fujian Province of China for Distinguished Young Scientists (2015J06002), the Youth Innovation Fund of Xiamen (3502Z20206045), and the program for New Century Excellent Talents in University of China (NCET-13-0495).

APPENDIX A: THE ANGULAR POSITION PROBABILITY DISTRIBUTION

In the process of spontaneous parametric down-conversion (SPDC), a strong pump beam (p) spontaneously generates a pair of signal (s) and idler (i) photons through an interaction with the nonlinear crystal, and its correlations of position and momenta are determined by the correlations of the pump field and the phase-matching function [53]. Here, we consider the ANG and OAM joint probability distribution of photon pairs that are converted from a spatially partial coherent pump beam. We assume the pump beam has the form of a monochromatic Gaussian Schell-model beam, and it is characterized by a cross-spectral density,

$$\Gamma(\boldsymbol{r}_1,\boldsymbol{r}_2)\sim\exp\left[-\frac{\boldsymbol{r}_1^2+\boldsymbol{r}_2^2}{4w^2}-\frac{(\boldsymbol{r}_1-\boldsymbol{r}_2)^2}{2l_c^2}\right]. \tag{A1}$$

Because the spatial coherence properties of the pump beam field get transferred to the spatial coherence properties of the down-converted two-photon field in SPDC [35], we replace $\boldsymbol{r}_1,\boldsymbol{r}_2$ with $(\boldsymbol{r}_s+\boldsymbol{r}_i)/2$, $(\boldsymbol{r}_s'+\boldsymbol{r}_i')/2$ in the cross-spectral function. The position density matrix of the degenerated photon pairs is given by

$$\hat{\rho}_{bi}(\boldsymbol{r}_s,\boldsymbol{r}_i;\boldsymbol{r}_s',\boldsymbol{r}_i')\sim\iiiint d\boldsymbol{r}_s d\boldsymbol{r}_i d\boldsymbol{r}_s' d\boldsymbol{r}_i'\Gamma(\boldsymbol{r}_s,\boldsymbol{r}_i;\boldsymbol{r}_s',\boldsymbol{r}_i') \times\cdot\chi(\boldsymbol{r}_s,\boldsymbol{r}_i)\cdot\chi^*(\boldsymbol{r}_s',\boldsymbol{r}_i')|\boldsymbol{r}_s,\boldsymbol{r}_i\rangle\langle\boldsymbol{r}_s',\boldsymbol{r}_i'|. \tag{A2}$$

$\chi(\boldsymbol{r}_s,\boldsymbol{r}_i)$ is the phase-matching function in position space and it is expressed as

$$\chi(\boldsymbol{r}_s,\boldsymbol{r}_i)\sim\sqrt{\frac{2k_p}{L(2\alpha-i)}}\exp\left[\frac{k_p(\boldsymbol{r}_s-\boldsymbol{r}_i)^2}{iL-2L\alpha}\right]. \tag{A3}$$

The phase-matching function is obtained by Fourier transform from the phase-matching function under a Gaussian approximation in momentum space just as Eq. (21) in Ref. [36]. It is noted that the position is a vector, and the density matrix can be expanded in polar coordinates. The $\boldsymbol{r}_s,\boldsymbol{r}_i$ can be decomposed with r_s, r_i, φ_s, φ_i, which is

$$\boldsymbol{r}_{s,i}=\begin{Bmatrix} r_{s,i}\cos\varphi_{s,i}\\ r_{s,i}\sin\varphi_{s,i}\\ 0\end{Bmatrix}. \tag{A4}$$

So, the elements of the density matrix in Eq. (A2) can be denoted in polar coordinates. The joint probability distribution can be defined by the diagonal elements of the density matrix, as $P(r_s,\varphi_s;r_i,\varphi_i)$. Thus the density matrix of the position of photon pairs can be simplified as

$$\begin{aligned}&\hat{\rho}_{bi}(r_s,r_i,\varphi_s,\varphi_i)\\ &\sim\int r_s dr_s\int r_i dr_i\int d\varphi_s\int d\varphi_i\frac{2k_p}{L\sqrt{1+4\alpha^2}}\\ &\times\exp\left[-\frac{1}{8w^2}\left[r_s^2+r_i^2+2r_sr_i\cos(\varphi_s-\varphi_i)\right]\right.\\ &\left.-\frac{4\alpha k_p}{L(1+4\alpha^2)}\left[r_s^2+r_i^2-2r_sr_i\cos(\varphi_s-\varphi_i)\right]\right]\\ &\times|r_s,r_i\rangle\otimes|\varphi_s,\varphi_i\rangle\langle r_s,r_i|\otimes\langle\varphi_s,\varphi_i|.\end{aligned} \tag{A5}$$

The density matrix of photon pairs consists of a radial and angular orientation freedom, where $|r\rangle$ is the complete orthonormal basis for the radial positions of photon pairs, and as such satisfies $\int rdr\langle r|r\rangle=1$. The radial positions and angular positions are noninteracting with each other, so the reduced density matrix of the angular positions can be obtained by the

partial trace of radial positions as

$$\hat{\rho}_{bi}(\varphi_s,\varphi_i)=\int rdr\langle r|\hat{\rho}_{bi}(r_s,r_i,\varphi_s,\varphi_i)|r\rangle \sim\sum_{n=0}^{\infty}\sum_{m=0}^{n}\int d\varphi_s\int d\varphi_i\frac{A}{4\alpha}\sqrt{\frac{B}{L}}\frac{1}{A+B}C_n^m \times\left(\frac{A+B}{2(A-B)}\right)^n e^{i(2m-n)(\varphi_s-\varphi_i)}|\varphi_s,\varphi_i\rangle\langle\varphi_s,\varphi_i|. \tag{A6}$$

Note that we have used the formulation $\frac{b}{x-a}=-\frac{b}{a}\sum_{n=0}^{\infty}(\frac{1}{a})^n x^n$ to simplify the density matrix of ANG. Here, $A=32w^2\alpha k_p$, $B=L(1+4\alpha^2)$. From Eq. (A6), one can see that the nonzero value of the density matrix exists with $\varphi_s=\varphi_i$, so the angular positions of photon pairs always retain a strong positive correlation. Then we have the angular position probability distribution $P(\varphi_s,\varphi_i)$ from Eq. (A6), as shown in Eq. (2). This is an analytical solution of the angular position probability distribution of photon pairs. The correlation of ANG of the signal and idler photons is independent of the transverse-coherence length l_c but can be controlled by the beam waist w and the nonlinear crystal length L, which is beyond the scope of this paper. So for the different pump coherence, the joint probability distribution of ANG is a constant and the variance should be zero theoretically. For an intuitive understanding, the transverse position correlations are independent of the pump coherence [36,45] so that we may determine a similar property of ANG through a Cartesian to polar coordinate transformation.

APPENDIX B: THE ORBITAL-ANGULAR-MOMENTUM PROBABILITY DISTRIBUTION

Under the condition of the radial position and angular position of the signal and idler photons remaining correlated, the phase-matching function in Eq. (A3) can be simplified as a constant. So, the simplified ANG density matrix of Eq. (A6) can be expanded in polar coordinates as

$$\hat{\rho}_{bi}(\varphi_s,\varphi_s')=\int rdr\langle r|\hat{\rho}_{bi}(r_s,r_s',\varphi_s,\varphi_s')|r\rangle \sim\int d\varphi_s\int d\varphi_s'\frac{2w^2l_c^2}{l_c^2+2w^2[1-\cos(\varphi_s-\varphi_s')]} \times|\varphi_s,\varphi_s\rangle\langle\varphi_s',\varphi_s'|. \tag{B1}$$

In order to obtain the joint probability distribution of OAM, we expand the density matrix of ANG in a complete orthonormal set of OAM states, which is

$$\tilde{\rho}(\ell_s,\ell_i)=\sum_{\ell_s,\ell_i}\langle\ell_s,\ell_i|\hat{\rho}_{bi}(\varphi_s,\varphi_s')|\ell_s,\ell_i\rangle \sim\int d\varphi_s\int d\varphi_s'\frac{2w^2l_c^2}{2w^2[1-\cos(\varphi_s-\varphi_s')]+l_c^2} \times\exp[i(\ell_s+\ell_i)\varphi_s-i(\ell_s+\ell_i)\varphi_s'], \tag{B2}$$

where we use $\langle\ell|\varphi\rangle=\exp[-i\ell\varphi]$ and $\tilde{\rho}(\ell_s,\ell_i)$ represents the diagonal elements of the OAM density matrix of photon pairs.

If we define

$$W(\varphi_s,\varphi_s')=-\frac{l_c^2}{\cos(\varphi_s-\varphi_s')-\left(1+\frac{l_c^2}{2w^2}\right)}, \tag{B3}$$

and since $\cos(\varphi_s-\varphi_s')\leqslant 1$, we can simplify this expression based on a formulation $\frac{b}{x-a}=-\frac{b}{a}\sum_{n=0}^{\infty}(\frac{1}{a})^n x^n$. Then we have $x=\cos(\varphi_s-\varphi_s')$, $a=(1+l_c^2/2w^2)$, $b=l_c^2$, so Eq. (B3) can be written as

$$W(\varphi_s,\varphi_s')=\frac{w^2}{2\beta^2+1}\sum_{n=0}^{\infty}(2\xi)^n\cos^n(\varphi_s-\varphi_s'), \tag{B4}$$

in which $\beta=\frac{w}{l_c}$ is used to describe the pump coherence property, and $\xi=\frac{\beta^2}{1+2\beta^2}$ is just for convenient notation. Then we expand the cosine to exponential and get

$$W(\varphi_s,\varphi_s')=\frac{w^2}{2\beta^2+1}\sum_{n=0}^{\infty}\sum_{m=0}^{n}C_n^m(\xi)^n\exp[i(2m-n)(\varphi_s-\varphi_s')]. \tag{B5}$$

We assume that $2m-n=k$ and obtain

$$W(\varphi_s,\varphi_s')=\frac{w^2}{2\beta^2+1}\sum_{j=0}^{\infty}C_{|k|+2j}^{j}(\xi)^{|k|+2j}\exp[ik(\varphi_s-\varphi_s')]. \tag{B6}$$

The diagonal elements of the OAM density matrix of photon pairs are expressed as

$$\tilde{\rho}(\ell_s,\ell_i)\sim\frac{w^2}{2\beta^2+1}\frac{1}{\sqrt{1-4\xi^2}}\left(\frac{2\xi}{\sqrt{1-4\xi^2}+1}\right)^{|\ell_s+\ell_i|}. \tag{B7}$$

So, the normalized probability distribution of OAM of the generated photon pairs is

$$\tilde{P}(\ell_s,\ell_i)=\frac{\sqrt{1-4\xi^2}}{1+2\xi}\left(\frac{2\xi}{\sqrt{1-4\xi^2}+1}\right)^{|\ell_s+\ell_i|}. \tag{B8}$$

From Eq. (B8), the joint probability distribution of OAM is relevant to the coherence length. One can then calculate the variances of OAM, $(\Delta\ell_i)^2=\sum_{\ell_i}\ell_i^2\cdot\tilde{P}(\ell_i|\ell_s=0)-[\ell_i\cdot\tilde{P}(\ell_i|\ell_s=0)]^2$. Based on the conditional probability $\tilde{P}(\ell_i|\ell_s=0)=\frac{\sqrt{1-4\xi^2}}{1+2\xi}(\frac{2\xi}{\sqrt{1-4\xi^2}+1})^{|\ell_i|}$, where we assume $\gamma=\frac{\sqrt{1-4\xi^2}}{1+2\xi}$, $a=\frac{2\xi}{\sqrt{1-4\xi^2}+1}$, we then obtain the analytical expression of the variances of OAM:

$$(\Delta\ell_i)^2=2\gamma\sum_{\ell_i=0}^{\infty}\ell_i^2a^{\ell_i}-4\gamma^2\left(\sum_{\ell_i=0}^{\infty}\ell_ia^{\ell_i}\right)^2 =\frac{2\beta^2(1+2\beta^2)}{1+4\beta^2}. \tag{B9}$$

By considering $\beta\ll 1$, Eq. (B9) can be simplified to $(\Delta\ell_i)^2\sim 2\beta^2$, while for $\beta\gg 1$, $(\Delta\ell_i)^2\sim\beta^2$. So it is clearly illustrated that the variance increases quadratically with β, which is also inversely proportional to the square of the coherence length l_c. One can know that, for a strong coherent pump beam, the correlation of OAM of photon pairs is strong but when the coherence length decreases, the entanglement of photon pairs decreases greatly, so varying the coherence length could be a useful tool to control the correlations of OAM of photon pairs.

[1] F. Flamini, N. Spagnolo, and F. Sciarrino, Rep. Prog. Phys. **82**, 016001 (2018).

[2] L. K. Shalm, E. Meyer-Scott, B. G. Christensen, P. Bierhorst, M. A. Wayne, M. J. Stevens, T. Gerrits, S. Glancy, D. R. Hamel, M. S. Allman, K. J. Coakley, S. D. Dyer, C. Hodge, A. E. Lita, V. B. Verma, C. Lambrocco, E. Tortorici, A. L. Migdall, Y. Zhang, D. R. Kumor, W. H. Farr, F. Marsili, M. D. Shaw, J. A. Stern, C. Abellán, W. Amaya, V. Pruneri, T. Jennewein, M. W. Mitchell, P. G. Kwiat, J. C. Bienfang, R. P. Mirin, E. Knill, and S. W. Nam, Phys. Rev. Lett. **115**, 250402 (2015).

[3] M. Giustina, M. A. M. Versteegh, S. Wengerowsky, J. Handsteiner, A. Hochrainer, K. Phelan, F. Steinlechner, J. Kofler, J.-A. Larsson, C. Abellán, W. Amaya, V. Pruneri, M. W. Mitchell, J. Beyer, T. Gerrits, A. E. Lita, L. K. Shalm, S. W. Nam, T. Scheidl, R. Ursin, B. Wittmann, and A. Zeilinger, Phys. Rev. Lett. **115**, 250401 (2015).

[4] S. J. Freedman and J. F. Clauser, Phys. Rev. Lett. **28**, 938 (1972).

[5] O. Kwon, K.-K. Park, Y.-S. Ra, Y.-S. Kim, and Y.-H. Kim, Opt. Express **21**, 25492 (2013).

[6] J. D. Franson, Phys. Rev. Lett. **62**, 2205 (1989).

[7] P. G. Kwiat, A. M. Steinberg, and R. Y. Chiao, Phys. Rev. A **47**, R2472 (1993).

[8] J.-P. W. MacLean, J. M. Donohue, and K. J. Resch, Phys. Rev. Lett. **120**, 053601 (2018).

[9] J. C. Howell, R. S. Bennink, S. J. Bentley, and R. W. Boyd, Phys. Rev. Lett. **92**, 210403 (2004).

[10] L. Chen, T. Ma, X. Qiu, D. Zhang, W. Zhang, and R. W. Boyd, Phys. Rev. Lett. **123**, 060403 (2019).

[11] A. Mair, A. Vaziri, G. Weihs, and A. Zeilinger, Nature (London) **412**, 313 (2001).

[12] J. Leach, B. Jack, J. Romero, A. K. Jha, A. M. Yao, S. Franke-Arnold, D. G. Ireland, R. W. Boyd, S. M. Barnett, and M. J. Padgett, Science **329**, 662 (2010).

[13] E. Yao, S. Franke-Arnold, J. Courtial, S. Barnett, and M. Padgett, Opt. Express **14**, 9071 (2006).

[14] S. Franke-Arnold, S. M. Barnett, E. Yao, J. Leach, J. Courtial, and M. Padgett, New J. Phys. **6**, 103 (2004).

[15] A. K. Jha, B. Jack, E. Yao, J. Leach, R. W. Boyd, G. S. Buller, S. M. Barnett, S. Franke-Arnold, and M. J. Padgett, Phys. Rev. A **78**, 043810 (2008).

[16] M. Mirhosseini, M. Malik, Z. Shi, and R. W. Boyd, Nat. Commun. **4**, 2781 (2013).

[17] M. Mirhosseini, O. S. Magaña-Loaiza, M. N. O'Sullivan, B. Rodenburg, M. Malik, M. P. Lavery, M. J. Padgett, D. J. Gauthier, and R. W. Boyd, New J. Phys. **17**, 033033 (2015).

[18] M. Malik, M. Mirhosseini, M. P. Lavery, J. Leach, M. J. Padgett, and R. W. Boyd, Nat. Commun. **5**, 3115 (2014).

[19] C. K. Law and J. H. Eberly, Phys. Rev. Lett. **92**, 127903 (2004).

[20] C. H. Monken, P. H. Souto Ribeiro, and S. Pádua, Phys. Rev. A **57**, 3123 (1998).

[21] K. W. Chan, J. P. Torres, and J. H. Eberly, Phys. Rev. A **75**, 050101(R) (2007).

[22] R. M. Gomes, A. Salles, F. Toscano, P. H. Souto Ribeiro, and S. P. Walborn, Phys. Rev. Lett. **103**, 033602 (2009).

[23] S. P. Walborn, C. H. Monken, S. Pádua, and P. H. S. Ribeiro, Phys. Rep. **495**, 87 (2010).

[24] J. Romero, D. Giovannini, M. McLaren, E. Galvez, A. Forbes, and M. Padgett, J. Opt. **14**, 085401 (2012).

[25] J. Romero, D. Giovannini, S. Franke-Arnold, S. M. Barnett, and M. J. Padgett, Phys. Rev. A **86**, 012334 (2012).

[26] E. V. Kovlakov, I. B. Bobrov, S. S. Straupe, and S. P. Kulik, Phys. Rev. Lett. **118**, 030503 (2017).

[27] Y. Chen, W. Zhang, D. Zhang, X. Qiu, and L. Chen, Phys. Rev. Appl. **14**, 054069 (2020).

[28] E. V. Kovlakov, S. S. Straupe, and S. P. Kulik, Phys. Rev. A **98**, 060301(R) (2018).

[29] S. Liu, Z. Zhou, S. Liu, Y. Li, Y. Li, C. Yang, Z. Xu, Z. Liu, G. Guo, and B. Shi, Phys. Rev. A **98**, 062316 (2018).

[30] S. Liu, Y. Zhang, C. Yang, S. Liu, Z. Ge, Y. Li, Y. Li, Z. Zhou, G. Guo, and B. Shi, Phys. Rev. A **101**, 052324 (2020).

[31] B. Baghdasaryan and S. Fritzsche, Phys. Rev. A **102**, 052412 (2020).

[32] D. Ghosh, T. Jennewein, P. Kolenderski, and U. Sinha, OSA Continuum **1**, 996 (2018).

[33] P. Boucher, H. Defienne, and S. Gigan, arXiv:2103.02320.

[34] X. Qiu, D. Zhang, W. Zhang, and L. Chen, Phys. Rev. Lett. **122**, 123901 (2019).

[35] A. K. Jha and R. W. Boyd, Phys. Rev. A **81**, 013828 (2010).

[36] E. Giese, R. Fickler, W. Zhang, L. Chen, and R. W. Boyd, Phys. Scr. **93**, 084001 (2018).

[37] S. V. Vintskevich, D. A. Grigoriev, and S. N. Filippov, Phys. Rev. A **100**, 053811 (2019).

[38] B. Kanseri and P. Sharma, J. Opt. Soc. Am. B **37**, 505 (2020).

[39] S. Joshi and B. Kanseri, Optik **217**, 164941 (2020).

[40] Y. Ismail, S. Joshi, and F. Petruccione, Sci. Rep. **7**, 12091 (2017).

[41] H. Defienne and S. Gigan, Phys. Rev. A **99**, 053831 (2019).

[42] L. Hutter, G. Lima, and S. P. Walborn, Phys. Rev. Lett. **125**, 193602 (2020).

[43] J. Galinis, M. Karpiński, G. Tamošauskas, K. Dobek, and A. Piskarskas, Opt. Express **19**, 10351 (2011).

[44] J. Galinis, G. Tamošauskas, and A. Piskarskas, Opt. Commun. **285**, 1289 (2012).

[45] W. Zhang, R. Fickler, E. Giese, L. Chen, and R. W. Boyd, Opt. Express **27**, 20745 (2019).

[46] S. P. Phehlukwayo, M. L. Umuhire, Y. Ismail, S. Joshi, and F. Petruccione, Phys. Rev. A **102**, 033732 (2020).

[47] L. Mandel and E. Wolf, *Optical Coherence and Quantum Optics* (Cambridge University Press, Cambridge, UK, 1995).

[48] T. Shirai, O. Korotkova, and E. Wolf, J. Opt. A: Pure Appl. Opt. **7**, 232 (2005).

[49] D. Dong and I. R. Petersen, IET Control Theory Appl. **4**, 2651 (2010).

[50] O. Lib, G. Hasson, and Y. Bromberg, Sci. Adv. **6**, eabb6298 (2020).

[51] D. d'Alessandro, *Introduction to Quantum Control and Dynamics* (CRC Press, Boca Raton, FL, 2007).

[52] S. Lloyd, Phys. Rev. A **62**, 022108 (2000).

[53] J. P. Torres, A. Alexandrescu, and L. Torner, Phys. Rev. A **68**, 050301(R) (2003).